Thermal Degradation of Starch in Production of Environmentally Benign Flocculants. 2. Experiments and Process Identification

János Gyenis,*,† Judit Dencs,‡ Gábor Nös,‡ and Gyula Marton‡

Research Institute of Chemical and Process Engineering and Department of Chemical Engineering, University of Pannonia, Egyetem u. 8, H-8200 Veszprem, Hungary

Experiments were carried out to produce biodegradable flocculants by phophorylation and heat treatment of corn starch at elevated temperatures in the dry state. The temporal change of molecular weight distribution was measured by HPSEC/MALLS/RI. To elucidate the mechanism and kinetics of degradation during this treatment a Markov-chain stochastic model was used. For this, five molecular weight intervals were defined between $>32 \times 10^6$ and 2×10^6 Da with exponentially decreasing spans. The probabilities of mass fraction transitions among these intervals at different processing temperatures were determined by fitting the calculated molecular weight distributions to the experimental data. Examining the transition probabilities between various MW intervals, it was concluded that degradation took place gradually by multiple splits of molecules, resulting in stepwise transition of fragments from higher intervals to lower ones. From the values of the transition probabilities between different molecular weight intervals, and considering the evolution of molecular weight distributions during the process, it was concluded that an end-scission mechanism did not play a role in the studied system under the applied conditions. The degradation probability of starch molecules diminished with decreasing molecular weight and increased with the temperature of treatment. These dependences were described by an exponential relationship.

Introduction

Starch is often used as a raw material to produce environmentally friendly industrial products, such as biodegradable polymers, chemicals, food additives, etc. An important example is to prepare flocculants by chemical or biochemical modification of starch. During the last two decades, several papers were published in this field, but because of the wide variety of objectives and methods, a number of questions remained open needing elucidation. In the majority of studies, mechanical or thermal treatments together with various reagents were used to modify and decompose starch molecules. Other works applied microorganisms or enzymes in aqueous phase at mild temperature to achieve the necessary transformations. Only a few papers were published on solid-phase treatment of starch in the dry state at relatively high temperatures.

Järnström et al.[1] prepared cationic flocculants from starch by oxidation with hypochlorite. The average molecular weight of the product was 2.6×10^5 Da with broad MW distribution. Deng et al.[2] produced flocculants with 3.2×10^5 Da average molecular weight from corn starch using microorganism in aqueous media at mild temperature. Pal et al.[3] have developed cationic flocculants by incorporating *N*-(3-chloro-2-hydroxypropyl)trimethyl ammonium chloride onto the starch molecules in the presence of NaOH. Bratskaya et al.[4] examined the efficiency of cationic flocculants obtained by chemical transformation of starch.

Wang and Wang[5] studied the structure and physicochemical properties of oxidized corn starch derivatives prepared by sodium hypochlorite. It was pointed out that cross-linking between starch molecules also took place during oxidation but this effect was overridden by degradation. Fiedorowicz et al.[6] emphasized that degradation is one of the most important targets of starch processing because it highly influences the behavior of the product during application. Thermal treatment and its combination with chemicals is the most common method of starch degradation.[7] Tomasik and Zaranyika[8] discussed the application of mechanical energy and other nonconventional methods such as irradiation with neutrons, X-ray, light, microwave, and ultrasound energy.

The majority of studies were rather application oriented, and only a few of them dealt with the fundamentals of the process. Van den Einde et al. applied heat and shear simultaneously in a pressurized mold,[9] in a shear cell,[10] and in a twin screw extruder.[11] It was concluded that the reduction of molecular weight in the temperature range of 85−110 °C was a time-independent process; i.e., the molecules were broken down instantaneously due to the high shear force. In extrusion cooking, the mechanical effects dominated over thermal effects.[12] The change of molecular size distribution in thermoplastic corn starch composites containing glycerol and cellulose fibers was studied by Carvalho et al.[13] in a mixer at 150−160 °C upon shear.

Several papers were published on the effect of chemicals on starch during thermal or mechanical treatment. Muhammad et al.[14] used sodium trimetaphosphate and sodium tripolyphosphate for chemical modification of sago starch in the semidry state at various pH levels at 130 °C as a maximum temperature. The progress of degradation was monitored by measuring physical properties only; i.e., no chemical analysis was used to determine the composition of products. Sang and Seib[15] studied the transformation of corn starch by simultaneous extrusion and phosphorylation at 110 °C and pH 11.5 to produce slowly digestible or resistant starch for nutritional purposes. The change of molecular weight distribution during this process was not examined.

Dencs et al. produced anionic flocculants by phosphorylation of starch in laboratory and pilot-plant scale.[16] The degradation of starch molecules realized at elevated temperatures in the dry state was monitored by measuring the molecular weight

* To whom correspondence should be addressed. E-mail: gyenis@mukki.richem.hu. Tel: : +36-88-624-032. Fax: +36-88-624-038.

† Research Institute of Chemical and Process Engineering.

‡ Department of Chemical Engineering.

10.1021/ie0613669 CCC: $37.00
Published on Web 10/31/2007

distributions versus time. Correlations were found between the flocculation characteristics, the bound phosphorus content, and the molecular weight distribution of the product. In another paper of this team,[17] it was emphasized that at least three types of transformations, namely, phosphorylation, degradation, and cross-linking, took place simultaneously during this process. The work reported here is a continuation of the investigation referred to above to elucidate the kinetics and mechanism of degradation.

In general, the scrutiny of examination in this field is in close relation with the method and resolution of measurements used to characterize the degradation products. Several studies examined only the change of intrinsic viscosity to estimate the progress of degradation,[3,10−12] but this did not allow deeper insight into the fundamentals of this process. Other researchers applied more sophisticated methods such as HPSEC,[6,16,17] HPAEC,[18] or gel permeation chromatography.[19] However, in the majority of works, the full potential of these methods was not utilized to elucidate the kinetics and mechanism of degradation. On the basis of HPSEC data, Fiedorowicz et al.[6] examined three molecular fractions only: amylopectin, intermediate, and amylase fractions. They pointed out that MW data above 10^8 Da could be considered as estimation only. Cai et al.[12] also emphasized the inaccuracy of HPLC-RI chromatograms.

Because the molecular weight distribution of starch derivatives has crucial importance in flocculation efficiency, the purpose of our work was to gain more knowledge on the kinetics and mechanism of degradation in order to optimize process conditions. In the study reported here, the effects of temperature and processing time were studied.

Experimental Section

To produce biodegradable anionic flocculants, corn waxy starch was modified by partial substitution of the OH groups in the anhydroglucose monomer units with phosphate groups in laboratory experiments.[16,17] The chemical reaction was carried out in the dry state at elevated temperatures, where phosphorylation and heat degradation took place simultaneously. Due to this latter, the molecular weight decreased from the original $(50-100) \times 10^6$ Da to a range of $(2-20) \times 10^6$ Da, depending on the temperature and duration of treatment.

At first, the native starch samples were impregnated with an aqueous solution of diammonium hydrogen phosphate and with a N-containing catalyst in mortar. Then the samples were dried and put into a block thermostat held at various temperatures for different lengths of time. The applied temperatures and processing times were changed from 135 to 150 °C, and from 5 to 270 min, respectively. Considering the reasonable combinations (the shortest treating times at low temperatures and long treating times at high temperatures were omitted), the effects of 108 different parameter combinations were investigated on the molecular weight distribution of the resulting products.

Materials. The raw material was Meritena 300 corn waxy starch supplied by Hungrana Ltd. The other reactants used for the experiments and analysis were bought from Merck AG, all analytical grade.

Methods. The reaction products were examined by measuring their molecular weight distributions. For this, starch phosphate samples of identical weights were suspended in distilled water (0.05 g in 5 mL of water) at 95 °C for 24 h and were analyzed by HPSEC/MALLS/RI as described by Meiczinger et al.[17] The HPLC system (LaChrom, Merck-Hitachi) had 2 × 30 cm × 7,8 mm × 8 μm PLaquagel-OH mixed columns (Polymer Laboratories). Injected samples had a volume of 5 μL containing 10 mg/mL reaction product. Conditions: elution, 1 mL/min pH 11 puffer; thermostat temperature, 30 °C; detectors, RI and MALLS (PD 2020, Precision Detectors).

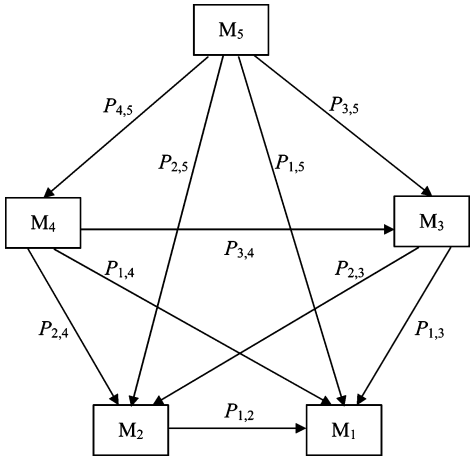

Figure 1. Structure of the applied stochastic model.

The soluble parts of samples, that is, the yield of the degradation process, were determined from the area below the RI chromatograms. The molecular weight distributions were calculated by Discovery 32 software from the chromatograms. At first, the obtained MW distributions were divided into 20 intervals of uniform width. Then, considering the reasonable scrutiny of modeling, and to moderate the stochastic variations of raw data, the whole molecular weight distribution including the nonsoluble part of products were regrouped to five MW intervals as will be shown below. Although this procedure resulted in somewhat smaller scrutiny compared to the simulation described in part 1 (previous paper in this issue), it proved to be enough to draw essential conclusions and was higher than used in some earlier studies.[6,9,10,12,14]

Applied Mathematical Model

The principles and details of the proposed stochastic model were discussed in part 1. In this second part, essentially the same model was applied to evaluate the experimental results, but using only five MW intervals. In Figure 1, these molecular weight ranges are represented by boxes, and the possible transitions among them are indicated by arrows. A $P_{j,i}$ element of matrix P in eq 1 gives the probability of transition from interval i to interval j in mass fraction per unit time.

$$P = \begin{vmatrix} P_{5,5} & 0 & 0 & 0 & 0 \\ P_{4,5} & P_{4,4} & 0 & 0 & 0 \\ P_{3,5} & P_{3,4} & P_{3,3} & 0 & 0 \\ P_{2,5} & P_{2,4} & P_{2,3} & P_{2,2} & 0 \\ P_{1,5} & P_{1,4} & P_{1,3} & P_{2,1} & 1 \end{vmatrix} \quad (1)$$

Matrix elements above the diagonal are zero because hypothetically transitions took place only from higher MW intervals to lower ones, due to degradation. If polymerization or cross-linking would also happen, $P_{j,i}$ denotes net transition, relating to the difference between the transitions caused by the two opposite processes.

In part 1 of this series, it was pointed out that any kind of division of the whole MW range (uniform or not uniform, linear or nonlinear) is allowed. Because the exact molecular weight distribution of the nonsoluble part of the samples (above 32×10^6 Da) was not known exactly, and the chromatograms of products had exponential MW scale, the transformation of the linear scale used in part 1 to exponentially decreasing MW

intervals seemed to be reasonable. For this study, the following intervals were defined:

$$M_5 \geq 32 \times 10^6 \text{ Da} > M_4 \geq 16 \times 10^6 \text{ Da} > M_3 \geq 8 \times 10^6 \text{ Da} > M_2 \geq 4 \times 10^6 \text{ Da} > M_1 \geq 2 \times 10^6 \text{ Da}$$

Because molecule fragments below 2×10^6 Da were observed in a few cases only (after long processing times at the highest temperatures) and in very low concentrations, further possible intervals below 2×10^6 Da were disregarded.

The state probability vector $p(t_n)$ in eq 2 corresponds to the expectable distribution of reaction products in intervals M_5-M_1 in mass fractions units, after processing time t_n.

$$p(t_n) = [p_5(t_n)\ \ p_4(t_n)\ \ p_3(t_n)\ \ p_2(t_n)\ \ p_1(t_n)\,] \tag{2}$$

The purpose of simulation described in part 1 was to elucidate the influence of different transition probability distributions on the state probabilities, i.e., on the expected molecular weight distributions of the products. The objective of this second part was just opposite; i.e., the transition probabilities $P_{j,i}$ had to be determined from measured MWD data.

The unknown transition probabilities $P_{j,i}$ were determined by fitting the estimated mass fractions $p_i(t_n)$ to the measured molecular weight distributions for the whole time period of treatment at given temperatures. For this purpose, calculations were carried out by solving a differential equation system composed of five equations in form of eq 3.

$$\frac{\mathrm{d}p_i}{\mathrm{d}t} = \sum_{k,k\neq i} (P_{i,k} \cdot p_k(t)) - p_i(t_n) \cdot \sum_{j,j\neq i} P_{j,i} \tag{3}$$

with the following initial distribution:

$$p(t_0) = [1\ \ 0\ \ 0\ \ 0\ \ 0\,] \tag{4}$$

Note that $P_{j,i}$ in eq 3 refer to the transitions from a given ith interval to any other interval (giving the expected mass fractions leaving interval M_i), while $P_{i,k}$ refer to the transitions to this ith interval from any other intervals (mass fractions entering interval M_i). For a given interval M_i ($5 \geq i \geq 1$), index k can vary in the range of $5 \geq k \geq 2$ if $k > i$, otherwise $P_{i,k}$ is zero, accordingly to the transitions shown in Figure 1. At the same time, j can vary in the range of $4 \geq j \geq 1$ if $j < i$; otherwise $P_{j,i}$ is zero.

The calculated molecular weight distributions were fitted to the measured mass fractions in intervals M_5-M_1 by optimizing 10 parameters ($P_{j,i}$ in matrix P) for the whole time of treatment (0−120, 0−210, or 0−240 min, depending on processing temperature). Although ModelMaker software that was applied to solve the differential equation system has parameter optimization facility, a trial-and-error method was used to find the best fit because this latter provided more freedom to adjust the calculated MWD profiles more or less separately from each other to the measured ones.

Degradation probabilities P_i in each molecular weight interval were determined from the calculated mass fraction transition probabilities $P_{j,i}$ by eq 5.

$$P_i = \sum_j P_{j,i} \tag{5}$$

Transition probabilities $P_{j,i}$ between different molecular weight intervals give information on the mechanism of degradation as will be shown later. On the other hand, knowing degradation probabilities P_i and their dependence on molecular weight and temperature are important for process characterization from the respect of the kinetics of degradation.

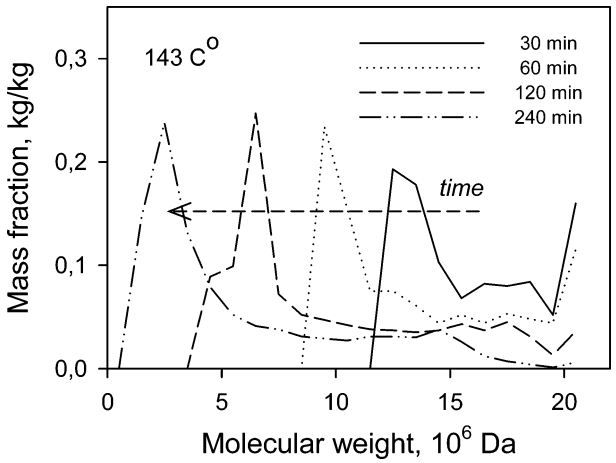

Figure 2. Shifts of the measured molecular weight distributions.

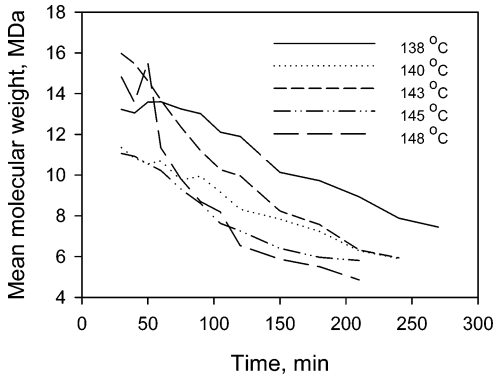

Figure 3. Change of the mean molecular weights.

Results and Discussion

The treatment of starch samples resulted in a gradually increasing proportion of soluble molecule fractions with decreasing molecular weights versus increasing temperature and reaction time. Figure 2 gives examples of the shifts of molecular weight distributions toward lower MW regions during treatment at 143 °C. The most important features seen here are the low region between two peaks measured in the first 60-min period of treatment and the sharp front at the lower end of the distribution. This behavior was observed at other processing temperatures, too. Although the smaller fluctuations on these diagrams were partially equalized by regrouping the raw distribution data to five molecular weight intervals M_5-M_1, the local minimums in the early stages of treatment remained observable as will be seen later.

Figure 3. shows examples of the steep decrease of the mean molecular weights of the soluble reaction products at five different temperatures versus processing time caused by degradation. Some contradictory data originated from the low solubility of higher MW fractions at the very beginning of treatment are not shown here. Figure 4 shows the increase of the proportion of water-soluble fractions versus time, i.e., the yield of the process at different reaction temperatures, determined from the areas below the RI chromatograms.

Panels a−c in Figure 5 show the temporal change of the relative amounts of molecule fragments in intervals M_4, M_3, and M_1, respectively, at various temperatures as examples. It should be emphasized that the weight fractions in intervals M_4-

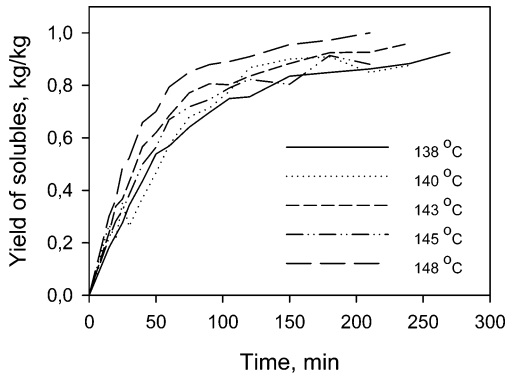

Figure 4. Yield of the soluble components.

M_1 were determined from the soluble part of the samples, while the insoluble fraction was ranked to M_5 supposing that the molecular weights in this part exceeded the lower limit of M_5 (32×10^6 Da). Panels a and b in Figure 5 illustrate that degradation products in the second highest (M_4, $(16-32) \times 10^6$ Da) and medium (M_3, $(8-16) \times 10^6$ Da) MW intervals have appeared already at the beginning of treatment. After a transitional increase, both fractions went through a maximum. Depending on the temperature, M_4 showed rapid decay approaching zero, while the relative amounts of M_3 reached nearly steady levels after 100−150 min of treatment. Note that the mass fraction of molecule fragments ranked to M_4 was fairly below M_3 during the whole time of treatment. This corresponds to the local minimums observed on the diagrams at the early stages of process and can be explained by direct transition from M_5 to M_3 or by the higher degradation rate of molecules in M_4 compared to M_3. Both explanations were confirmed by the proposed model as will be seen later.

Figure 5c shows the change of concentrations in the lowest MW fraction M_1 versus time. Apart from the data obtained at the highest temperature, 150 °C (not shown here), degradation products in this fraction (MW = $(2-4) \times 10^6$ Da) appeared only after a long time delay, this latter increasing with decreasing temperature.

Determination of the Transition Probabilities. Using the proposed stochastic model, calculations were carried out to determine the transition probabilities $P_{j,i}$. For this, these parameters were varied systematically to fit the calculated molecular weight distribution to the measured data. To evaluate the extent of deviations, the less squares method was used in a trial-and-error optimization process. Besides monitoring the standard error of fit for the whole data set at given temperatures, the deviation was also watched for each molecular weight interval separately.

The surface plot in Figure 6 gives an example for the time evolution of molecular weight distribution along intervals M_5-M_1 at 145 °C obtained by fitting the calculated distributions to the experimental data. Intersections of this surface with vertical planes parallel to the front horizontal axis characterize the molecular weight distributions after different processing times, while intersections with planes perpendicular to this axis show the change of concentration in given MW intervals versus time. Notice that similarly to Figure 2 a local minimum is seen here around $i = 4$ (see the arrow) indicating that the applied model well reflects the behavior observed experimentally.

Statistical Tests. The goodness of fit and statistical significance was checked by ANOVA and *F*-tests (*p*-values), also examining the pattern of residuals. These tests were carried out for the whole data set gained for all molecular weight intervals and separately for each molecular weight interval obtained at

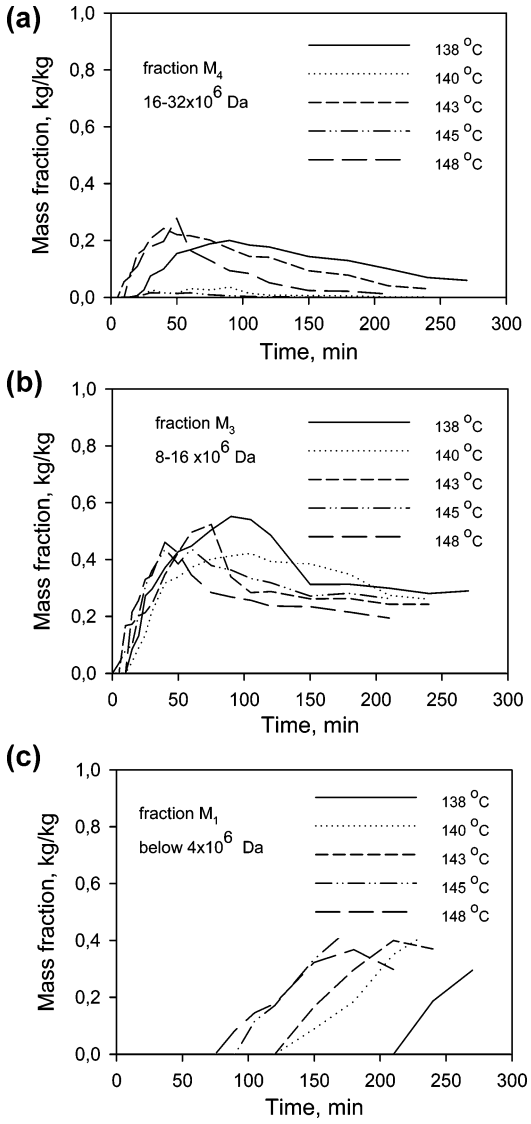

Figure 5. Change the amount of different MW fractions, (a) M_1, (b) M_3, and (c) M_4.

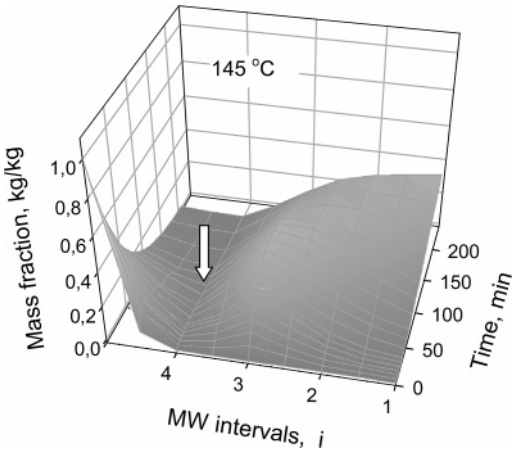

Figure 6. Calculated molecular weight distribution at 145 °C.

the given temperatures. The results showed reasonable fits and confirmed the adequacy of the proposed model. As regards *F*-tests, the *p*-values determined at different temperatures were generally between 0.0000 and 0.0048, i.e., far below the commonly accepted $p < 0.05$ significance level. Only three exceptions were found when the *F*-test failed because of the lack of significant change in a given MW interval. This latter

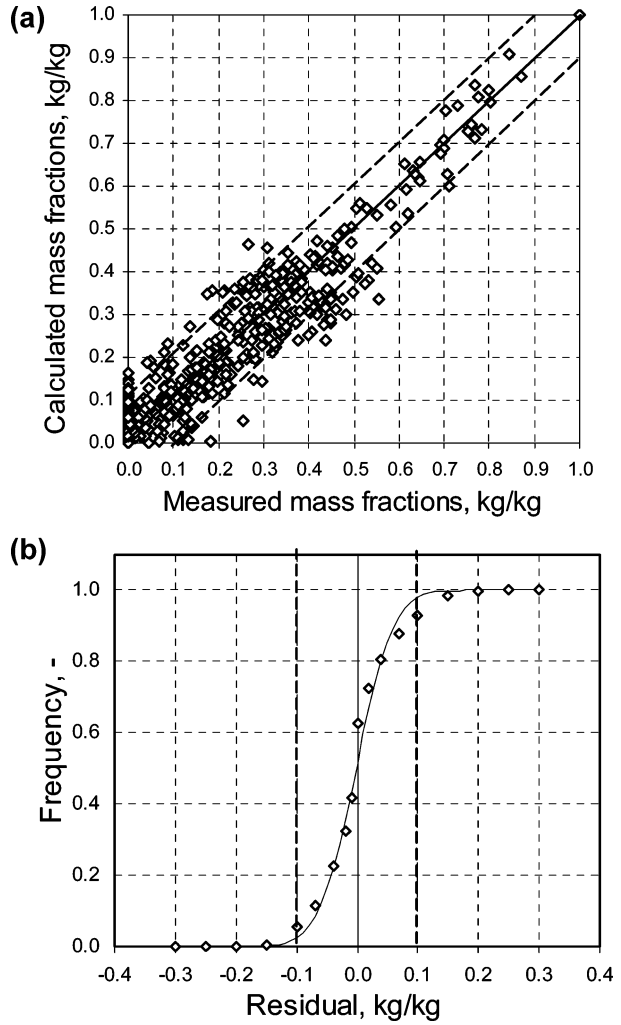

Figure 7. Comparison of the experimental and calculated data, (a) Scattering around the measured values and (b) distribution of residuals.

was caused by low transitions to that MW interval (e.g., to M_1 at 125 °C) or by high transition from this interval to all other ones (e.g., from M_4 at 145 and 150 °C). In two other cases, the significance test just passed ($p \cong 0.049 < 0.05$) because of the relatively higher fluctuations of experimental data in given MW intervals (concentrations in M_3 and M_2 at 148 °C).

The goodness of fit and the adequacy of the model were also checked by calculating the standard error of estimates separately for the seven processing temperatures. The values of standard error were 0.055, 0.067, 0.067, 0.046, 0.056, 0.080, 0.053 (5.5, 6.7, 6.7, 4.6, 5.6, 8.0, 5.3%) for the data set obtained at 135, 138, 140, 143, 145, 148, and 150 °C, respectively. Notice that in addition to the reasonably low values of these errors, they do not differ from each other significantly. The standard error determined for the whole data set (for all temperatures and processing times) was 0.0622 (6.2%). The comparison of the measured and calculated data shown in Figure 7a also indicates good agreement. The distribution of residuals seen in Figure 7b is symmetrical around zero and was well approximated by normal distribution function with parameters $\mu = -0.02$, $\rho = 0.05$ shown by continuous line. The 95% of the residuals were between ± 0.010, shown by dashed line in Figure 7a,b.

Dependence of the Transition Probabilities on the Molecular Weight and Temperature. The transition probabilities between various MW intervals that gave the best fits are shown in Figure 8a−c at temperatures 135, 143, and 148 °C, respectively, as examples. To understand these diagrams, let us consider a column at the crossing point of given *i*th and *j*th grid lines in the bottom plane. The height of data column at this point gives the value of transition probability $P_{j,i}$, which corresponds to the expected mass fraction transition from the *i*th to the *j*th molecular weight interval per minute. The row of columns aligned parallel to axis *j* at an *i*th grid line gives the transition probabilities from that *i*th interval to all other intervals. The columns along a *j*th grid line (parallel to axis *i*) give the transition probabilities toward this *j*th interval from other intervals. At last, the columns on the left side (marked as "total") are the sum of transition probabilities from given *i*th intervals to all other *j*th intervals. According to eq 5, these columns correspond to degradation probabilities P_i as a function of the molecular weight range of the splitting molecules.

Comparing probability values $P_{j,i}$ to each other, information was obtained on the mechanism of degradation:

1. Transitions from M_5 to Lower MW Intervals. From the original starch ranked into the highest MW interval ($>32 \times 10^6$ Da, $i = 5$) transitions are most probable to M_3 ($(8-16) \times 10^6$ Da, $j = 3$) at all temperatures studied. Notice that the probabilities shown in these figures refer to direct transitions from a given interval to other ones. For example $P_{3,5}$ gives the chance of transition from M_5 to M_3 directly and not via M_4. From the diagrams, it can be seen that direct transitions from M_5 to M_4 ($(16-32) \times 10^6$ Da, $j = 4$) also have fairly high probability, but transition to M_2 ($(4-8) \times 10^6$ Da, $j = 2$) may occur at higher temperatures only. Direct transition from M_5 to M_1 (MW $= (2-4) \times 10^6$ Da, $j = 1$) practically has no chance.

Interpretation. The molecular weight of the original starch was $(50-100) \times 10^6$ Da. Therefore, at the very beginning of the process, the degradation of starch molecules ranked to interval M_5 could produce fragments above 32×10^6 Da. It was therefore supposed that, after an initial period, interval M_5 contained molecules in the whole range of $(32-100) \times 10^6$ Da. According to Figure 8a−c, transition from M_5 to M_3 has the highest probability and depending on temperature considerable transition may occur from M_5 to M_4 and M_2. This can happen if molecules in interval M_5 split to 2−20 fragments. Let us see an example; if a molecule in M_5 with a molecular weight of 80×10^6 Da splits to 3−5, 6−10, or 11−20 parts of similar lengths, it causes transitions to M_4, M_3, or M_2, respectively. Similar transitions take place if a molecule of 40×10^6 Da MW breaks to 2, 3−5, or 6−10 pieces. If the fragments have different sizes, the number of transferred fragments to M_4, M_3, or M_2 should be less than supposed above for case of uniform sizes.

More precise data could be obtained on the size and number of fragments by examining transitions between narrower MW fractions. However, considering the information obtained until now, it can be stated that splitting took place inside the chain of molecules, and the length of fragments was not less than the lower limit of M_2 (i.e., was above 4×10^6 Da). Because no transition took place from interval M_5 into M_1 or below (i.e., fragments with molecular weight less than 2×10^6 Da were detected in a few cases and negligible amounts only), it can be stated that end-scission mechanism did not play a role in the studied process.

2. Transitions from M_4 to Lower MW Intervals. Molecule fragments entering M_4 (MW $= (16-32) \times 10^6$ Da) from M_5 have high probability for further degradation, mainly toward M_2 (MW $= (4-8) \times 10^6$ Da) as is seen from the data column in Figure 8a−c at $i = 4$ and $j = 2$ for all temperatures. At higher temperatures, transition from M_4 to interval M_3 (MW $= (8-16) \times 10^6$ Da, $j = 3$) was also possible with increasing probability. Because of the rapid degradation of molecules in

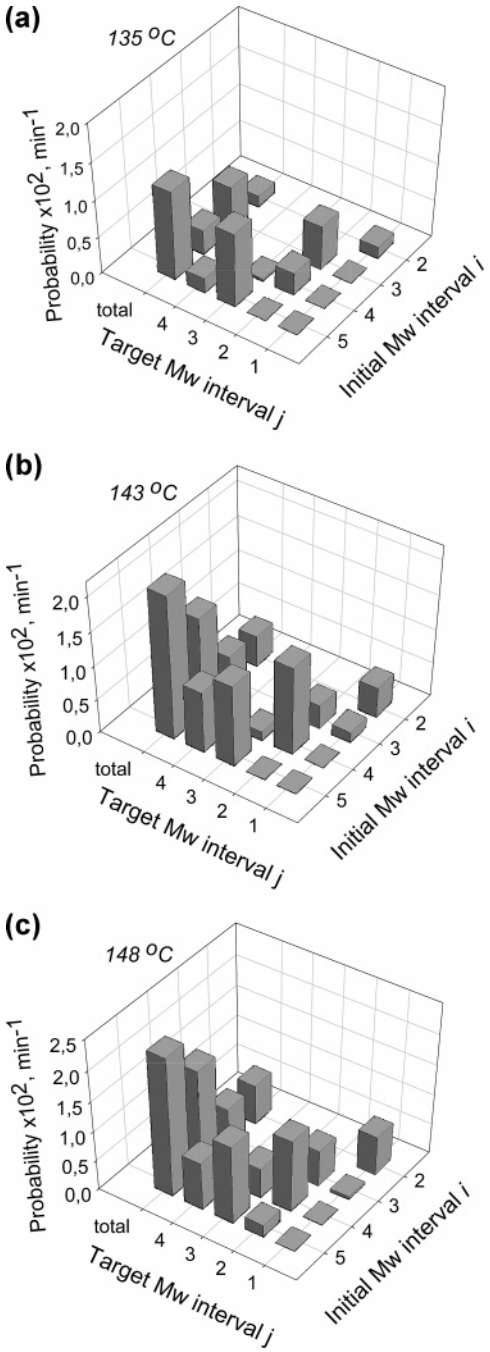

Figure 8. Transition probabilities at various temperatures determined by the model.

M_4, and due to the relatively low transition from M_5 to M_4, no too high accumulation was observed in M_4 (see Figure 5a).

Possible Mechanism. Transitions from M_4 to M_2 and M_3 could take place by splitting the molecules to two to seven pieces, supposing similar lengths. If, for example, a molecule of MW $= 30 \times 10^6$ Da splits only to two pieces, the resultant fragments will have molecular weights of 15×10^6 Da each, meaning that both pieces will be transferred to interval M_3. If it splits to seven pieces, we obtain fragments of $\sim$4,3 $\times 10^6$ Da MWs, just above the lower limit of M_2. Because practically no transition took place from M_4 to M_1, this also confirms that end-scission mechanism had no role in the decomposition of molecules in the studied system.

3. Transitions from M_3 to Lower MW Intervals. Panels a-c in Figure 8 show that transitions from M_3 (MW $= (8-16) \times 10^6$ Da) are possible to M_2 (MW $= (4-8) \times 10^6$ Da) and

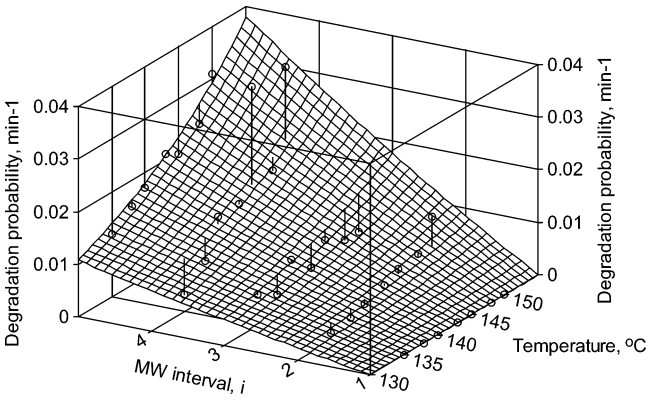

Figure 9. Degradation probabilities vs temperature and MW intervals.

with minor probability to M_1 (MW $= (2-4) \times 10^6$ Da). It means that molecules in interval M_3 can split most probably around the middle of the chain producing two fragments. However, there is certain probability of splitting to three or four pieces causing transition to M_1.

4. Transitions from M_2 to M_1. Looking at the data column at $i = 2$ and $j = 1$, it is seen that transition from M_2 (MW $= (4-8) \times 10^6$ Da) to M_1 (MW $= (2-4) \times 10^6$ Da) is the only possibility to leave interval M_2. This can happen only if molecules in M_2 split to two or three pieces.

Summarizing these experiences, it looks like breakage of molecules goes on stepwise, by their split to several pieces, causing gradual transitions from higher MW intervals to lower ones. It was seen from the data that transitions from a higher MW interval were most probable to the next and second lower intervals, and there were no direct transitions from intervals M_5-M_3 to M_1 or below; i.e., no end-scission took place in this process.

Degradation Probabilities. The data column on the left side of the diagrams in Figure 8a−c shows the change of degradation probabilities P_i (see eq 5) along different MW intervals at various temperatures. Comparing these data, a decreasing tendency of degradation probabilities can be observed with decreasing molecular weights, but a significant rise took place with increasing temperature. To elucidate the relationship between these variables, all P_i values were plotted in one diagram versus molecular weight and temperature. Various functions (linear, polynomial, and exponential) were tried to describe these data, employing the TableCurve 3D software (SPSS Inc.) for regression and statistical analysis. The best fit shown in Figure 9 was obtained by exponential correlation as

$$P_i = a \cdot e^{b \cdot T} \cdot (i-1) e^{c \cdot (i-1)} \qquad (6)$$

with parameters $a = 3.55 \times 10^{-12}$, $b = 5.04 \times 10^{-2}$ and $c = 3.77 \times 10^{-2}$.

In spite of the scattering of data points around the fitted surface on this plot, it was concluded that the probability of degradation increased exponentially with the temperature of treatment and declined with the decrease of the molecular weight. It was supposed that the main reason of data scattering was the stochastic nature of the studied process. Use of index i instead of the mean molecular weights of intervals M_i was more reasonable because these latter values were changing during the process and had some uncertainty especially in M_5.

The standard error of regression was ± 0.0050 ($\sim \pm 14\%$ of the highest P_i value). This seems to be acceptable, but a few data had higher deviation as is seen in Figure 9. The influence of temperature and molecular weight interval on the degradation

probabilities proved to be significant as was shown by *F*-test ($F = 51.35 >> F_{crit} = 3.29$, $p = 0.0000$).

The relations discovered by this study helped to optimize the process conditions to obtain flocculants with required molecular weight distribution. Temperatures between 143 and 145 °C resulted in a suitable degree of degradation within reasonable treatment time. Namely, at 143 °C, after 120-min treatment, ≃73 wt % product was found within the range of $(4-16) \times 10^6$ Da, with no observable fraction above 20×10^6 Da and below 4×10^6 Da. At 145 °C, after 105 min, already 86 wt % product was below 16×10^6 Da, but in this case, 12 w% was already below 4×10^6 Da.

Summary and Conclusions

Experiments and calculations were carried out to elucidate the mechanism and kinetics of degradation during phosphorylation of starch in the dry state at elevated temperatures. For interpretation of the experimental data, a Markov-chain stochastic model developped in the first part of this study was used. The whole molecular range of the original starch and its degradation products between $>32 \times 10^6$ and 2×10^6 Da was divided into five intervals with exponentially decreasing spans. Transition probabilities among these MW intervals were estimated by fitting the MW distributions calculated by the model to the measured data. Statistical analysis on the influence of molecular weight intervals of the splitting molecules and processing time on the resulted molecular weight distribution of the products showed good agreement at all processing temperatures with low standard errors and high significance level.

From the values of transition probabilities between different MW intervals, it was deduced that starch degradation took place by multiple splits inside the chains transferring their fragments from higher to lower MW intervals step by step. Under the studied conditions, no end-scission mechanism was detected.

In studying the influence of process conditions on the probability of degradation, it was concluded that this latter increased exponentially with increasing temperature. It was seen that starch molecules in higher molecular weight intervals degraded with higher probabilities, also meaning that susceptibility of starch derivates for degradation decreased continuously during the process. To describe the effect of these variables, an exponential relationship was proposed. The applied stochastic model and the evaluation of experimental data helped us to find optimal conditions to produce flocculants from starch with suitable molecular weight distribution.

Nomenclature

M_i = *i*th molecular weight interval, characterized by its mean molecular weight, Da

$P_{j,i}$ = mass fraction transition probability from an *i*th to a *j*th molecular weight interval, min^{-1}

P_i = degradation probability of molecules in the *i*th molecular weight interval, min^{-1}

P = transition probability matrix (eq 1)

$p(t_n)$ = state probability vector describing the expectable distribution of material in different molecular weight intervals at time t_n, kg/kg

$p_i(t_n)$ = state probability or expectable mass fraction in the *i*th molecular weight interval at time t_n, kg/kg

t = time, min

T = absolute temperature (eq 6), K

dp_i/dt = differential change of probability p_i, min^{-1}

Acknowledgment

The authors acknowledge the financial support of the Hungarian National Research and Development Program (Grant No. NKFP 2001-3/072).

Literature Cited

(1) Järnström, L.; Lason, L.; Rigdahl, M. Flocculation in kaolin suspensions induced by modified starches 1. Cationically modified starch - effects of temperature and ionic strength. *Colloids Surf., A: Physicochem. Eng. Aspects* **1995**, *104* (2−3) 191−205.

(2) Deng, S.; Yu, G.; Ting, Y. P. Production of a bioflocculant by Aspergillus parasiticus and its application in dye removal. *Colloids Surf., B: Biointerfaces* **2005**, *44* (4), 179−186.

(3) Pal, S.; Mal, D.; Singh, R. P. Cationic starch: an effective flocculating agent. *Carbohydr. Polym.* **2005**, *59* (4), 417−423.

(4) Bratskaya, S.; Schwarz, S.; Liebert, T.; Heinze, T. Starch derivatives of high degree of functionalization, 10. Flocculation of kaolin dispersions. *Colloids Surf. A: Physicochem. Eng. Aspects* **2005**, *254* (1−3), 75−80.

(5) Wang, Y-J.; Wang, L. Physicochemical properties of common and waxy corn starches oxidized by different levels of sodium hypochlorite. *Carbohydr. Polym.* **2003**, *52* (3), 207−217.

(6) Fiedorowicz, M.; Tomasik, P.; Lii, C. Y. Degradation of starch by polarised light. *Carbohydr. Polym.* **2001**, *45* (1), 79−87.

(7) Tomasik, P.; Wiejak, S.; Palasinski, M. The thermal decomposition of carbohydrates. Part II. The decompensation of starch. *Adv. Carbohydr. Chem. Biochem.* **1989**, *47*, 279−343.

(8) Tomasik, P.; Zaranyika, M. F. Nonconventional methods of modification of starch. *Adv. Carbohydr. Chem. Biochem.* **1995**, *51*, 243−320.

(9) van den Einde, R. M.; Bolsius, A.; van Soest, J. J. G.; Janssen, L. P. B. M.; van der Goot, A. J.; Boom, R. M. The effect of thermomechanical treatment on starch breakdown and the consequences for process design. *Carbohydr. Polym.* **2004**, *55* (1), 57−63.

(10) van den Einde, R. M.; Akkermans, C.; van der Goot, A. J.; Boom, R. M. Molecular breakdown of corn starch by thermal and mechanical effects. *Carbohydr. Polym.* **2004**, *56* (4), 415−422.

(11) van den Einde, R. M.; van der Veen, M. E.; Bosman, H.; van der Goot, A. J.; Boom, R. M. Modeling macromolecular degradation of corn starch in a twin screw extruder. *J. Food Eng.* **2005**, *66* (2), 147−154.

(12) Cai, W.; Diosady, L. L.; Rubin, L. J. of Wheat Starch in a Twin-screw Extruder. *J. Food Eng.* **1995**, *26*, 289−300.

(13) Carvalho, A. J. F.; Zambon, M. D.; Curvelo, A. A. S.; Gandini, A. Size exclusion chromatography characterization of thermoplastic starch composites 1. Influence of plasticizer and fibre content. *Polym. Degrad. Stab.* **2003**, *79* (1), 133−138.

(14) Muhammad, K.; Hussin, F.; Man, Y. C.; Ghazali, H. M.; Kennedy, J. F. Effect of pH on phosphorylation of sago starch. *Carbohydr. Polym.* **2000**, *42* (1), 85−90.

(15) Sang, Y.; Seib, P. A. Resistant starches from amylose mutants of corn by simultaneous heat-moisture treatment and phosphorylation. *Carbohydr. Polym.* **2006**, 63, 167−175.

(16) Dencs, J.; Nos, G.; Dencs, B.; Marton, G. Investigation of Solid-Phase Starch Modification Reactions. *Trans. IchemE, Part A* **2003**, *81*, 1−5.

(17) Meiczinger, M.; Dencs, J.; Marton, G.; Dencs, B. Investigation of Reactions Occurring at Starch Phosphorylation. *Ind. Eng. Chem. Res.* **2005**, *44* (25), 9581−9585.

(18) Blennow, A.; Bay-Smidt, A. M.; Wischmann, B.; Olsen, C. E.; Møller, B. L. The degree of starch phosphorylation is related to the chain length distribution of the neutral and the phosphorylated chains of amylopectin. *Carbohydr. Res.* **1998**, *307* (1−2), 45−54.

(19) Willett, J. L. Millard and M. M. Jasberg, B. K. Extrusion of waxy maize starch: melt rheology and molecular weight degradation of amylopectin, *Polymer* **1997**, *24*, 5983−5989.

Received for review October 24, 2006
Revised manuscript received September 4, 2007
Accepted September 7, 2007

IE0613669